

The WRP component of the WAVE-1 complex attenuates Rac-mediated signalling

Scott H. Soderling*†, Kathleen L. Binns†‡§, Gary A. Wayman¶, Stephen M. Davee*, Siew Hwa Ong‡, Tony Pawson§ and John D. Scott*#

*Howard Hughes Medical Institute, Vollum Institute, 3181 Sam Jackson Park Road, Portland, Oregon 97239-3098, USA

‡Samuel Lunenfeld Research Institute, Mount Sinai Hospital, 600 University Avenue, Toronto, Ontario M5G 1X5, Canada

§Department of Molecular and Medical Genetics, University of Toronto, Toronto, Ontario M5G 1X5, Canada

¶Vollum Institute, 3181 Sam Jackson Park Road, Portland, Oregon 97239-3098, USA

#e-mail: scott@ohsu.edu

†These authors contributed equally to this work

Published online: 25 November 2002; DOI: 10.1038/ncb886

WAVE-1, which is also known as Scar, is a scaffolding protein that directs actin reorganization by relaying signals from the GTPase Rac to the Arp2/3 complex. Although the molecular details of WAVE activation by Rac have been described, the mechanisms by which these signals are terminated remain unknown. Here we have used tandem mass spectrometry to identify previously unknown components of the WAVE signalling network including WRP, a Rac-selective GTPase-activating protein. WRP binds directly to WAVE-1 through its Src homology domain 3 and specifically inhibits Rac function *in vivo*. Thus, we propose that WRP is a binding partner of WAVE-1 that functions as a signal termination factor for Rac.

Actin reorganization is a bidirectional process that orchestrates complex cellular events such as cell migration, neurite extension and bud growth in yeast^{1,2}. The WASP family of scaffolding proteins, WASP, N-WASP and WAVE, participate in these processes by relaying signals from Rho-family GTPases to the actin remodelling machinery^{3–6}. This is achieved by the dynamic assembly of multiprotein complexes that include signalling molecules, actin-binding proteins and the Arp2/3 complex, a group of seven proteins that control actin assembly at the leading edge^{7,8}. WAVE-1 also recruits the cyclic-AMP-dependent protein kinase (PKA) and the tyrosine kinase Abl in response to signals that activate the small GTPase Rac⁹. Other WAVE-interacting proteins include profilin and IRSp53, an adaptor protein that may link WAVE-2 to active Rac^{10,11}.

In a screen for WAVE-binding partners from mammalian tissue, we immunoprecipitated WAVE complexes from rat brain extracts. Silver stain detected several unique protein bands in the WAVE immune complex (Fig. 1a, lane 2) that were not present in control immunoprecipitations (Fig. 1a, lane 1). WAVE-specific bands were excised from the gel, digested by trypsin and sequenced by nano-electrospray tandem mass spectrometry. Amino-acid sequences obtained from collision-induced dissociation of selected peptide ions (Fig. 1b) were used to search nonredundant sequence databases. Several peptides were obtained for most proteins (Table 1).

We identified unambiguously WAVE-1 and seven potential binding partners. These proteins included cytoskeletal components such as α -tubulin, spectrins α II and β III, Src homology domain 3 (SH3)-containing adaptor proteins such as the Abl-kinase-interacting proteins Abi-1 and Abi-2, and SNIP, a protein that interacts

with SNAP-25 (synaptosomal-associated protein of relative molecular mass (M_r) 25,000)¹². The identities of these proteins are consistent with a role for WAVE-1 in cytoskeletal reorganization. For example, Abi-1 and Abi-2a are localized to regions of actin polymerization, such as protruding lamellipodia and filopodia tips¹³, and Abi-1 has been implicated in Rac activation by the Sos1 guanine nucleotide-exchange factor (GEF)¹⁴.

In addition to these known polypeptides, we also isolated seven peptides from a sequence (KIAA0411) encoding a Rho-family GTPase-activating protein (GAP; Table 1 and Fig. 1c). An expressed sequence tag (EST) encompassing the KIAA0411 sequence was obtained and the remainder of the coding region was amplified from human brain complementary DNA by reiterative 5' rapid amplification of cDNA ends (RACE) to generate a transcript of 8,415 base pairs (bp), encoding a protein of 1,076 amino acids (Fig. 1c, d). Analysis of the sequence identified an FCH (Fes, Cip4 homology) domain between residues 11 and 120, a GAP domain between residues 496 and 646 with similarity to Rho-family GAP proteins, and an SH3 domain between residues 723 and 777 (Fig. 1d). The mouse orthologue is 98% identical to the human protein. We called this protein WRP (for WAVE-associated RacGAP protein). Three related Rho-family GTPases have also been identified in GenBank; srGAP1 (accession code XM051143), KIAA0456 (AB007925) and C1 rhoGAP (NM001666).

Northern blot analysis of human tissues with a WRP probe detected two messenger RNA species of roughly 8.5 kilobases (kb) and 7.4 kb, which, in common with WAVE-1 (ref. 10), are expressed predominantly in the brain (Fig. 1e). The dual transcript lengths may indicate that there are alternative splice variants of WRP. Further northern blot analysis identified overlapping expression patterns for the WAVE-1 and WRP mRNAs in most of the brain regions that we examined (Fig. 1f).

The interaction of the WRP and WAVE-1 proteins in rat brain was confirmed by reciprocal co-immunoprecipitation experiments (Fig. 1g, h). Immunoprecipitation of WAVE resulted in the co-precipitation of WRP as detected by western blot using an antibody generated against an WRP peptide (Fig. 1g, lane 1), whereas control experiments with pre-immune serum were negative (Fig. 1g, lane 2). This result was confirmed by immunoprecipitation of WRP, which resulted in the co-precipitation of WAVE-1 (Fig. 1h, lane 1). Control experiments using pre-immune serum were negative (Fig. 1h, lane 2). Immunocytochemical characterization in mouse embryonic fibroblasts detected the colocalization of epitope-tagged

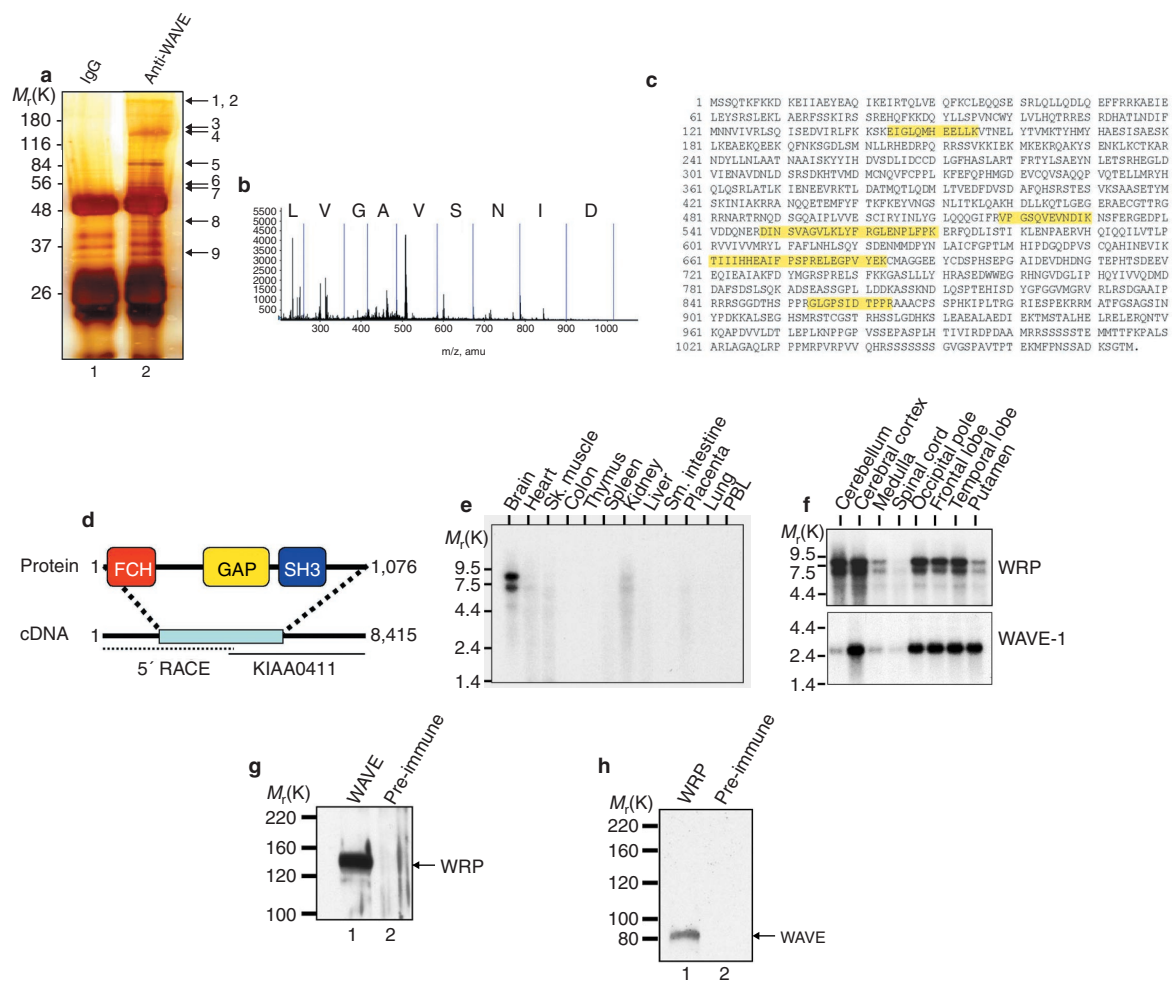


Figure 1 The WAVE-1 protein network and characterization of WRP. WAVE-1 immune complexes were isolated from rat brain extracts. **a**, Pre-immune (lane 1) and WAVE immunoprecipitations (lane 2) were resolved by SDS-PAGE and detected by silver staining. Bands specific to the WAVE immune complexes were numbered, excised from the gel and digested with trypsin; the resulting peptides sequenced by nano-electrospray tandem mass spectrometry. **b**, Representative example of data obtained from band 4 contained in EST clone KIAA0411 (WRP). **c**, Amino-acid sequence of WRP. Each peptide identified by mass spectrometry is highlighted.

d, Domain structure of WRP, showing the location of an FCH domain, a region with homology to Rho-family GAP proteins and an SH3 domain. **e**, Tissue expression of WRP determined by northern blot using KIAA0411 as a probe. PBL, peripheral blood leukocyte. **f**, Expression pattern of WRP mRNA in selected brain regions (top) was compared with that of WAVE-1 (bottom). **g**, **h**, Confirmation of the WRP-WAVE interaction by reciprocal co-immunoprecipitation techniques. **g**, Immunodetection of WRP in WAVE complexes from rat brain. **h**, Immunodetection of WAVE in WRP complexes from rat brain.

WRP with endogenous WAVE and actin at the cell cortex (Supplementary Information). Collectively, these results suggest that WRP is a Rho-family GAP protein that contains an FCH and SH3 domain and is a component of the WAVE-1 signalling complex.

Wild-type WRP associated with WAVE-1 when both proteins were expressed in HEK293 cells (Fig. 2a, top panel, lane 1). By contrast, mutation of a conserved tryptophan in the WRP SH3 domain (Trp 757) to alanine, which perturbs peptide recognition¹⁵, abolished interaction with WAVE-1 (Fig. 2a, lane 2; top). Control experiments confirmed that equal quantities of protein were expressed in each sample (Fig. 2a, bottom). Thus, the SH3 domain of WRP is necessary for its interaction with WAVE-1. *In vitro* pull-down experiments using the WRP SH3 domain fused to glutathione S-transferase (GST-WRP-SH3) specifically captured recombinant WAVE-1, showing that these proteins interact directly (Fig. 2b, lane 3). Overlay experiments verified that GST-WRP-SH3 associates selectively with a rat brain protein that migrates with the same mobility as WAVE-1 (Fig. 2c).

We used the GST-WRP-SH3 fusion protein as a probe to screen a solid-phase peptide array of overlapping 20-residue sequences (each displaced by three amino acids), spanning the polyproline region between residues 258 and 492 of WAVE-1 (Fig. 2d). Binding of GST-WRP-SH3 was detected by immunoblot using a monoclonal antibody against GST. Specific binding was detected at two sites between residues 320 and 332 and residues 420 and 433 of WAVE-1 (Fig. 2d). These sequences contain a core of seven or eight prolines with a carboxy-terminal leucine (Fig. 2d). Both WRP-binding sites are distinct from the SH3 recognition motif for c-Abl, which is also contained in this region^{9,16}. Independent confirmation of the peptide array analysis was provided by evidence that a WAVE deletion mutant lacking both of these binding sites (WAVEΔ1Δ2) did not interact with WRP when both proteins were expressed in HEK293 cells (Fig. 2e, top panel, lane 2). Thus, we propose that the SH3 domain of WRP binds directly to proline-rich sequences located within residues 320–332 and 420–433 of WAVE-1.

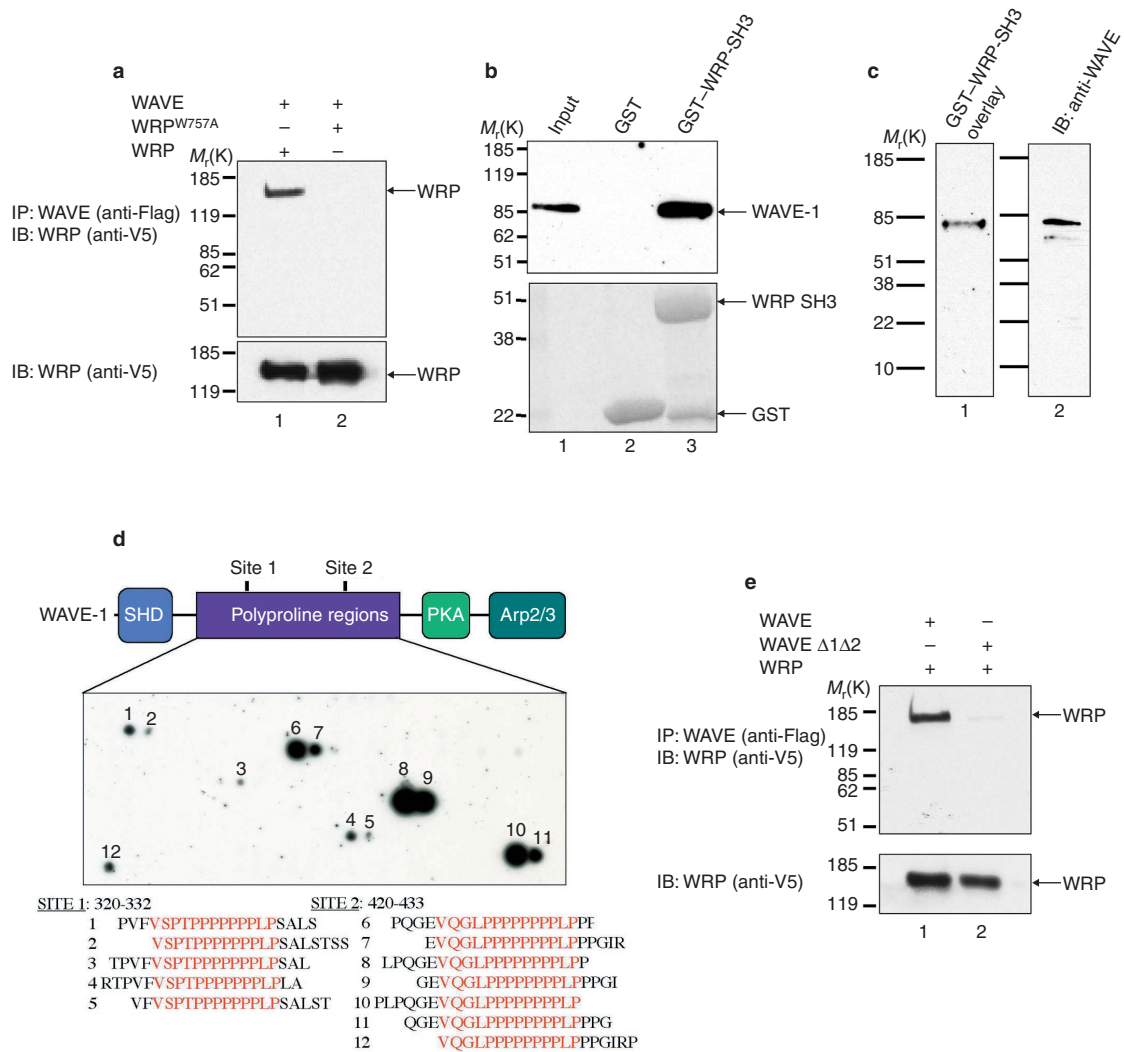


Figure 2 Defining the interactive surfaces on WRP and WAVE-1. **a**, Flag-tagged WAVE and V5-tagged WRP were expressed in HEK293 cells. WAVE was immunoprecipitated from cells expressing wild-type WRP (lane 1) or WRP^{W757A} (lane 2). Top, co-purification of recombinant WRP was assessed by immunoblot using antibodies against V5. Bottom, expression of both forms of WRP was assessed by immunoblot. **b**, A GST fusion protein of the WRP SH3 domain binds recombinant WAVE-1. Top, immunodetection of a WAVE-1 input (extract from WAVE-1 transfection; lane 1), a GST control (lane 2) and eluate from the GST-WRP-SH3 pull down (lane 3). Bottom, detection of the GST fusion proteins by Coomassie blue. **c**, Rat brain extracts were screened by overlay procedure using the GST-WRP-SH3 fusion protein as a probe. Left, solid-phase binding was assessed by immunoblot for GST. Right, detection of WAVE-1 in rat brain extracts. **d**, Peptide array analysis of the WRP-binding sites on WAVE-1. Top, structure of WAVE-1, showing the Scar homology domain (SHD),

a polyproline region, the PKA-anchoring site, an Arp2/3-binding site and the two WRP-binding sites. Middle, the GST-WRP-SH3 fusion protein was used as a probe to screen an array of overlapping 20-residue peptides spanning the polyproline region (residues 258–492) of WAVE-1. Solid-phase binding was assessed by immunoblot through antibodies against GST. The WRP-binding peptides are numbered. Data from three staggered peptide arrays are shown. Bottom, alignment of WRP-binding sequences with common residues highlighted in red. **e**, Flag-tagged WAVE-1 and V5-tagged WRP were expressed in HEK293 cells. Top, immune complexes were isolated from cells expressing wild-type WAVE (lane 1) or the WAVEΔ1Δ2 deletion mutant that lacks both WRP-binding sites (lane 2). Co-purification of the recombinant WRP form was assessed by immunoblot for V5-tagged WRP. Bottom, expression of WRP assessed by immunoblotting.

WAVE-1 is thought to reorganize cortical actin in response to signals from the small GTPase Rac, but not the closely related molecules Rho or Cdc42 (ref. 10). Because WRP is predicted to be a GTPase-activating protein^{17,18}, we tested whether it possessed Rac-selective GAP activity. *In vitro* activity measurements showed that recombinant WRP stimulates the intrinsic GTPase activity of Rac (Fig. 3a) but has no effect on the activities of Rho or Cdc42 (Fig. 3b), indicating that WRP may be a Rac-selective GAP. Control experiments using Pak-1 and Rhotekin pull-down assays also suggested that WRP regulates Rac, whereas WRP lacking a GAP domain (WRP^{ΔGAP}) does not (see Supplementary Information).

To test the hypothesis that WRP regulates Rac in a more physiological context, we examined whether WRP can modulate Rac-mediated neurite outgrowth in cerebellar granular neurons^{19,20}. Transfection of WRP reduced neurite outgrowth in cerebellar granular neurons by 59 ± 6% (*n* = 89) as compared with control transfections (Fig. 3c, d, h, i), whereas transfection of WRP^{ΔGAP} did not alter neurite outgrowth (Fig. 3e, i). Neurite outgrowth was also reduced by 58 ± 7% (*n* = 72) in cerebellar granular neurons transfected with Rac^{T17N}, a dominant-negative form of the GTPase (Fig. 3f, i). Likewise, transfection of the WRP^{W757A} mutant that does not bind WAVE still abolished neurite outgrowth, suggesting that

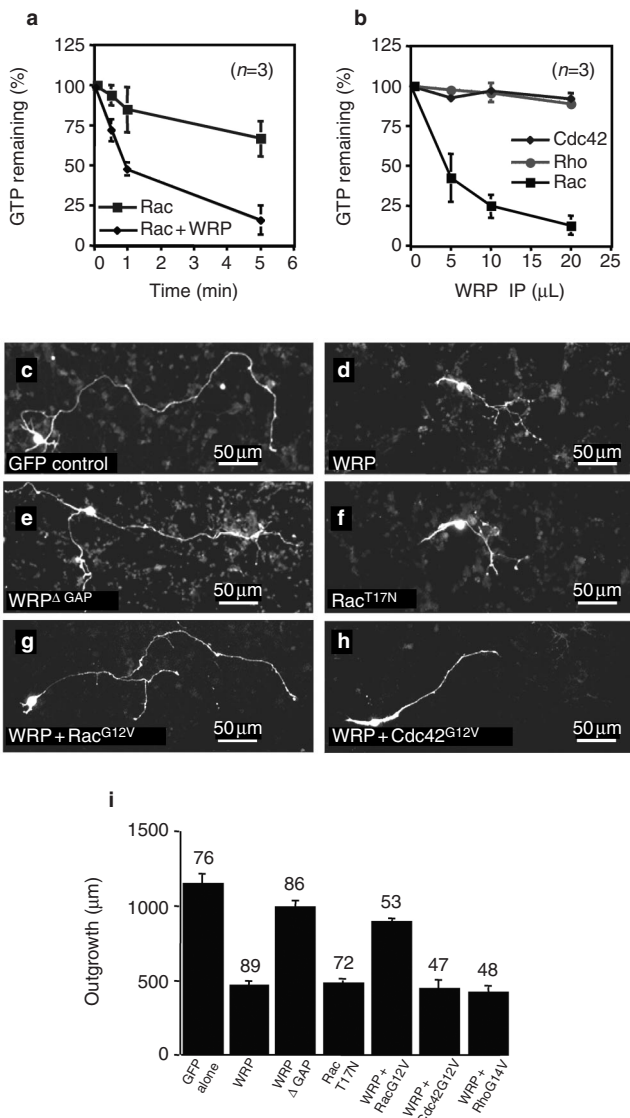


Figure 3 WRP is a Rac-selective GTPase-activating protein. **a**, *In vitro* measurement of Rac GTPase activity in the presence (diamonds) or absence (squares) of recombinant WRP. GTPase activity (percentage of GTP remaining) was measured over time. Data are the mean \pm s.e.m. of three experiments. **b**, WRP activity was measured in the presence of purified Rac (squares), Rho (circles) or Cdc42 (diamonds). GTPase activity was measured in increasing amounts (μ l) of WRP. Data are the mean \pm s.e.m. from three experiments. **c–h**, Effect of WRP on Rac-mediated neurite outgrowth in cerebellar granular neurons. Neurons were transfected with a GFP control (**c**); GFP and WRP (**d**); GFP and WRP Δ GAP, a deletion mutant lacking the GAP domain (**e**); GFP and Rac^{T17N}, a dominant-negative effector of Rac function (**f**); GFP, WRP and Rac^{G12V}, a constitutively active form of Rac (**g**); and GFP, WRP and Cdc42^{G12V}, a constitutively active form of Cdc42 (**h**). Scale bars, 50 μ m. **i**, Extent of neurite outgrowth (μ m) 3 d after transfection with the indicated cDNAs, as assessed by fluorescent visualization and digitization. Data are the mean \pm s.e.m. from three independent experiments. The number of cells analysed in each condition is indicated above each column.

GAP activity predominates over proximity in this overexpression assay (data not shown).

Additional experiments suggested that neurite outgrowth was restored on co-transfection of WRP with Rac^{G12V}, an active form of the GTPase (Fig. 3g, i). By contrast, co-transfection of WRP with

active forms of Cdc42 or Rho reduced neurite outgrowth by $62 \pm 14\%$ ($n = 47$) and $64 \pm 9\%$ ($n = 48$), respectively (Fig. 3h, i), indicating that only constitutively active Rac can rescue the effect of WRP. Although it is plausible that WRP may also possess GAP activity towards an as yet unidentified GTPase, taken together our data indicate that WRP functions to attenuate Rac signalling events selectively in neurons.

A long-standing issue in studies of the superfamily of small GTPases is how each GAP protein is directed specifically to the correct Rho-family GTPase. Here we have identified a GAP protein for a Rho-family GTPase that is directed toward its substrate through association with WAVE-1, a scaffolding protein and a known downstream target of Rac. Notably, the recruitment of Rho-family GTPase regulatory molecules may represent a general function for WASP family members. For example, WAVE recruits Abi-1 and WRP, signalling proteins that are implicated in Rac activation¹⁴ and inhibition, respectively. In addition, N-WASP, which is activated directly by Cdc42, associates with intersectin-1, a GEF that is specific for Cdc42 (ref. 21). Both examples indicate that WASP family members recruit regulatory proteins for Rho-family GTPases and, taken together, they raise the possibility that Rac or Cdc42 activity may be coordinated by GAP and GEF activities located in the same multiprotein complex. An analogous system may also exist in yeast, as a WAVE homologue, Las17, has been shown to bind Rgd1, a yeast GAP with similarities to WRP. Together, these proteins seem to regulate Arp2/3-mediated actin polarization (M. Evangelista and C. S. Boone, personal communication).

A similar biochemical approach has been used to identify other WAVE-1-interacting partners, including bovine orthologues of PIR121 (a p53-inducible mRNA), Nap125 (a protein that associates with the adaptor protein Nck) and heat-shock protein HSPC300 (ref. 22). It has been proposed that Rac regulation of actin polymerization involves the dissociation of active WAVE-1 from this heterotetrameric complex. In light of this new information, we propose that WRP may provide a signal termination component to shut down Rac-mediated transduction through the WAVE-1 complex.

In summary, we have identified several WAVE-associated SH3 proteins that are involved in either signal transduction (PKA⁹, Abl⁹, Abi-1 and Abi-2) or signal termination (WRP). We have also detected four cytoskeletal components, including tubulin and spectrin, that may link the WAVE complex to cytoskeletal structures other than actin. Given the number of WAVE-binding partners that have been identified so far, it seems likely that the combinatorial assembly of individual signalling networks may provide a mechanism for specifying the assembly and function of filamentous actin structures. Future studies will be directed at establishing which of these binding partners influence the activation state of WAVE and respond to signals that flow through this multiprotein complex. □

Methods

Immunoprecipitation experiments

Soluble tissue extracts were prepared from frozen rat brains (Pel Freeze, Rogers, AK) by Dounce homogenization in lysis buffer (25 mM HEPES, 150 mM NaCl, 0.5% Triton X-100, 1 mM EDTA, 1 mM 4-(2-aminoethyl)-benzenesulphonyl fluoride, 1 mM benzamide, 2 μ g ml⁻¹ pepstatin and 2 μ g ml⁻¹ leupeptin) and centrifugation at 38,000g twice for 1 h at 4 °C. WAVE immune complexes were isolated by incubation of samples (4 ml) with polyclonal antibodies (V059 or V0101) and captured on agarose beads conjugated to protein A (Upstate Biotechnology, Cleveland, OH). We eluted the bound proteins with Laemmli sample buffer and resolved them by SDS-PAGE and silver staining.

Mass spectrometry

Proteins were reduced, alkylated and digested with trypsin in-gel as described²³. Tryptic peptides were extracted from the gel, desalted using ZipTip desalting columns (Millipore, Bedford, MA), equilibrated in 5% formic acid, washed with equilibration buffer and eluted in a solution of 5% formic acid and 60% methanol.

We carried out tandem mass spectrometry analysis using a nano-electrospray source (Protana A/S) coupled to a high-performance hybrid quadrupole time-of-flight API QSTAR pulsar (MDS-Sciex, Concord, ON, Canada). After tryptic ion candidates were identified, product ion spectra were generated by collision-induced dissociation. For product ion scans, the collision energy was determined experimentally. Sequence and mass information of the peptides were used to screen the NRDB and dbEST databases. We searched the databases using the Mascot MS/MS search engine (Matrix Science, London, UK).

Table 1 Proteins associated with WAVE identified by tandem mass spectrometry

Gel band†	Protein	Accession number	Sequenced peptides	Peptide mass‡
1	Spectrin α II	gij 179106	• IEDLGAAMEEALILDNK • LAILAAHEPAIQGVLDTGK	1860.926 2062.081
2	Spectrin β III	gij 3550974	• NHYAAEEISEK	1290.596
3	SNIP	gij 6693834	• LLEETQAELLK • DINRLEETQAELLK	1284.98 1783.27
4	WRP (Kiaa0411)	gij 3334418	• VPGSQVEVNIK • DINSVAGVLK • DINSVAGVLKLYFR • TIIHHEAIFPSPR • ELEGPVYEK • GLGPSIDTPPR • GLENPFLK • EIGLQMHEELLK	1283.67 1014.57 1593.89 1629.90 1062.52 1108.59 1013.55 1438.75
5	WAVE-1	gij 4927210	• SSTIQDQLFDRK • LSVSVTLQDPK	1564.78 1185.58
6	Abi-1	gij 7839526	• WAIYDYTK • HAPANMERPVR • KPEDYTVLDDVGHGVK • ALIESYQLNTR	1070.58 1365.58 1755.88 1306.78
7	Abi-2	gij 7839524	• HAPANLERPVR • ALFDSYTNLER	1347.88 1327.64
8	WAVE-1 (degradation product)	gij 4927210	• SSTIQDQLFDRK • LSVSVTLQDPK	1564.78 1185.58
9	α -Tubulin	gij 4929136	• DVNAAIATIK	1014.38

*Each protein was identified in three separate WAVE immunoprecipitations using two different antibodies against WAVE

†Gel band numbers refer to those shown in fig. 1a

‡The peptide mass is given in Daltons

Antibodies

We raised a rabbit antibody against residues 475–494 of WRP (CGTTRGRNRNARTRNQDSGQA). V059 is a rabbit antibody raised against full-length WAVE-1. V0101 is a peptide antibody raised against residues 223–248 of WAVE-1 (KHIEVANGPASHFETRPQTYVDHMDG).

cDNA cloning and mutagenesis

A cDNA encoding the whole WRP coding region was generated by ligating the 5' end of WRP to KIAA0411. The 5' end of the WRP coding region was generated by 5' RACE using a 5' adaptor oligonucleotide and a 3' gene-specific oligonucleotide from the beginning of the KIAA0411 sequence. Transcripts of 2,690 bp were generated by polymerase chain reaction with reverse transcription (RT-PCR) from two independent pools of human brain RNA using Superscript II (Invitrogen, Carlsbad, CA). Two independent clones were sequenced. To generate a full-length cDNA, we ligated a *Bam*H1/*Bgl*II restriction fragment from KIAA0411 into a pCRII-TOPO vector containing the 5' coding region of WRP that had been linearized by cutting with *Bam*H1. The coding region of WRP was subsequently cloned into the mammalian expression vector pCDNA3.1/V5-His-TOPO and sequenced. Mutagenesis of WRP and WAVE was done using the QuickChange kit (Stratagene, La Jolla, CA). WAVE Δ 1 Δ 2 was expressed in equal quantities as WAVE, as determined by immunoblot of extracts (data not shown).

GST overlay and auto-spot peptide synthesis

GST–WRP–SH3 was incubated with peptide arrays at a concentration of 0.4 ng ml⁻¹ in 5% milk overnight. The filter was washed in Tris-buffered saline/Tween-20 (TBST; three times for 10 min each) and the bound GST fusion protein was detected by overlay using antibodies against GST (Santa Cruz, Biotechnology, Santa Cruz, CA). Peptide arrays were synthesized on cellulose paper using an Auto-Spot Robot ASP 222 (AbiMed, Langenfeld, Germany) as described²⁴. After synthesis, the amino termini were acetylated with 2% acetic acid anhydride in dimethyl formamide. The peptides were then deprotected by a 1 h treatment with dichloromethane:trifluoroacetic acid (1:1), containing 3% tri-isopropylsilane and 2% water.

GTPase assays

GTPase hydrolysis was measured as described²⁵. Briefly, recombinant GTPases were loaded with ³²P-GTP at 30 °C in buffer containing 20 mM Tris-HCl (pH 7.6), 0.1 mM dithiothreitol (DTT), 25 mM NaCl and 4 mM EDTA. We terminated loading by adding MgCl₂ to a final concentration of 17 mM. GTPase reactions were done at 30 °C in a volume of 30 μ l in buffer containing 20 mM Tris-HCl

(pH 7.6), 0.1 mM DTT, 1 mM GTP and 1 mg ml⁻¹ bovine serum albumin. Hydrolysis reactions were terminated by removing 5- μ l aliquots from the hydrolysis reaction and diluting them in 1 ml of ice-cold buffer containing 50 mM Tris-HCl (pH 7.6), 50 mM NaCl and 5 mM MgCl₂. Remaining bound GTP was measured by scintillation counting after the samples had been filtered through pre-wetted nitrocellulose.

Recombinant WRP was partially purified by immunoprecipitation using antibodies against V5. We defined GAP activity as the stimulation of intrinsic GTP hydrolysis measured with Rac in the presence of WRP versus Rac alone. For WRP specificity experiments, equal amounts (0.3 μ g per reaction) of bacterially expressed and purified Rac, Cdc42 or Rho were used, as determined by Coomassie-stained gels and Bradford assay, and each GTPase was assayed to determine that each protein was active (intrinsic GTP hydrolysis over time). Specificity assays were restricted to 30 s to limit the contribution of intrinsic GTPase activity.

Neurite outgrowth measurements

We prepared cerebellar granule cell cultures from dissociated cerebellar cortices of postnatal day 6–8 Sprague Dawley rats by using papain dissociation (Worthington Biochemicals, Lakewood, NJ). Granule cells were plated at 2–4 \times 10⁵ cells per cm² on borosilicate glass coverslips coated with poly-D-lysine (300K; Sigma, St Louis, MO) and grown in Neurobasal A media (Invitrogen) supplemented with 2% B27, 4% fetal bovine serum (FBS), 0.5 mM L-glutamine, 25 mM KCl, and 5 μ M AraC. For studies on neurite extension, the cells were maintained in 4% FBS and 2% B27 plus a high potassium ion concentration for 12–96 h and then transfected. Cells were cultured an additional 3 d before neurite outgrowth was measured by fluorescent visualization using OpenLab 3.0 (Improvision, Coventry, UK).

Accession numbers

The GenBank numbers for human and mouse WRP are AF464189 and AF496547, respectively. All protein interactions listed in this paper have been submitted to the Biomolecular Interaction Database (<http://www.bind.ca/>) with the following interaction identity numbers: spectrin α II, 12368; spectrin β III, 12369; SNIP, 12366; WRP, 12361; Abi-1, 12364; Abi-2, 12365; α -tubulin, 12367.

RECEIVED 4 JULY 2002, REVISED 4 OCTOBER 2002, ACCEPTED 18 OCTOBER 2002, PUBLISHED 25 NOVEMBER 2002.

- Hall, A. *Science* 279, 509–514 (1998).
- Adams, A. E. & Pringle, J. R. *J. Cell Biol.* 98, 934–945 (1984).
- Mullins, R. D. *Curr. Opin. Cell Biol.* 12, 91–96 (2000).

4. Machesky, L. M. & Insall, R. H. *Curr. Biol.* **8**, 1347–1356 (1998).
5. Takenawa, T. & Miki, H. *J. Cell Sci.* **114**, 1801–1809 (2001).
6. Bear, J. E., Krause, M. & Gertler, F. B. *Curr. Opin. Cell Biol.* **13**, 158–166 (2001).
7. Welch, M. D. *Trends Cell Biol.* **9**, 423–427 (1999).
8. Higgs, H. N. & Pollard, T. D. *Annu. Rev. Biochem.* **70**, 649–676 (2001).
9. Westphal, R. S., Soderling, S. H., Alto, N. M., Langeberg, L. K. & Scott, J. D. *EMBO J.* **19**, 4589–4600 (2000).
10. Miki, H., Suetsugu, S. & Takenawa, T. *EMBO J.* **17**, 6932–6941 (1998).
11. Miki, H., Yamaguchi, H., Suetsugu, S. & Takenawa, T. *Nature* **408**, 732–735 (2000).
12. Chin, L. S., Nugent, R. D., Raynor, M. C., Vavalle, J. P. & Li, L. *J. Biol. Chem.* **275**, 1191–1200 (2000).
13. Stradal, T. *et al. Curr. Biol.* **11**, 891–895 (2001).
14. Scita, G. *et al. Nature* **401**, 290–293 (1999).
15. Erpel, T., Superti-Furga, G. & Courtneidge, S. A. *EMBO J.* **14**, 963–975 (1995).
16. Rickles, R. J. *et al. EMBO J.* **13**, 5598–5604 (1994).
17. Rittinger, K. *et al. Nature* **388**, 693–697 (1997).
18. Boguski, M. S. & McCormick, F. *Nature* **366**, 643–654 (1993).
19. Luo, L., Jan, L. & Jan, Y. N. *Perspect. Dev. Neurobiol.* **4**, 199–204 (1996).
20. Luo, L., Jan, L. Y. & Jan, Y. N. *Curr. Opin. Neurobiol.* **7**, 81–86 (1997).
21. Hussain, N. K. *et al. Nature Cell Biol.* **3**, 927–932 (2001).
22. Eden, S., Rohatgi, R., Podtelejnikov, A. V., Mann, M. & Kirschner, M. W. *Nature* **418**, 790–793 (2002).
23. Shevchenko, A., Wilm, M., Vorm, O. & Mann, M. *Anal. Chem.* **68**, 850–858 (1996).
24. Frank, R. & Overwin, H. *Methods Mol. Biol.* **66**, 149–169 (1996).
25. Self, A. J. & Hall, A. *Methods Enzymol.* **256**, 67–76 (1995).

ACKNOWLEDGEMENTS

We thank L. Langeberg for help preparing the manuscript; R. Mouton for technical assistance; C. S. Boone and M. Evangelista for sharing unpublished data and for critical review of the manuscript; and T. R. Soderling for support. This work was supported by grants from the National Institutes of Health, the Canadian Institutes of Health Research (CIHR), the National Cancer Institute of Canada (NCIC) and the Ontario R&D Challenge Fund (J.D.S., T.P. & G.A.W.). T.P. is a CIHR Distinguished Scientist. K.L.B. is supported by a National Science and Engineering Research Council of Canada (NSERC)/MDS-Sciex Industrial Postgraduate Scholarship. S.H.O. is supported by a postdoctoral fellowship from the National Medical Research Council of Singapore. Supplementary Information accompanies the paper on www.nature.com/naturecellbiology. Correspondence and requests for materials should be addressed to J.D.S.

COMPETING FINANCIAL INTERESTS

The authors declare they have no competing financial interests.

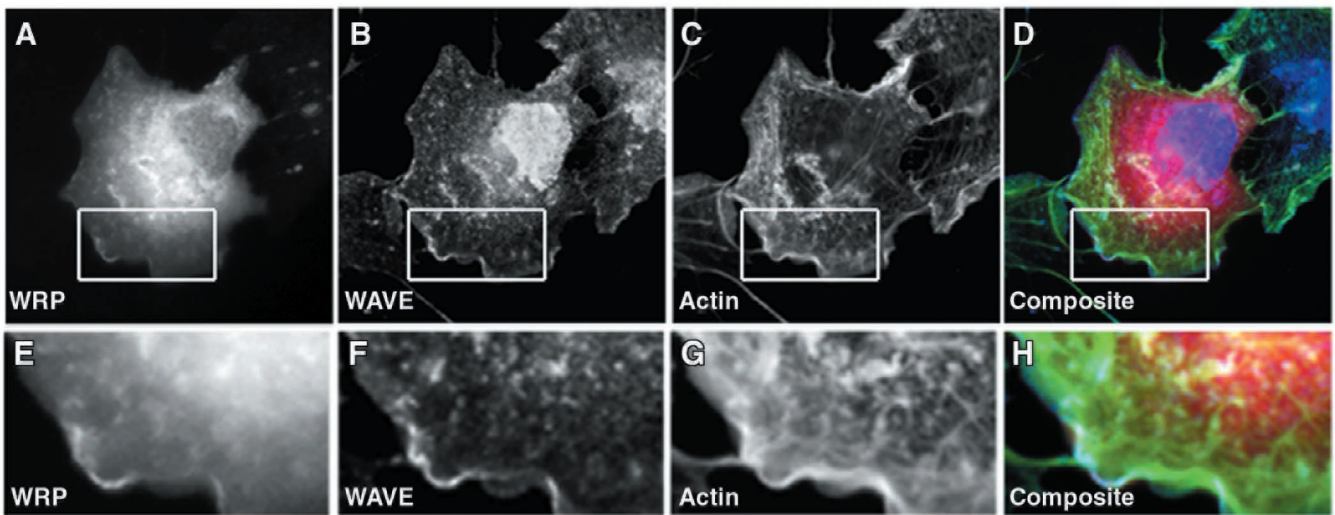


Figure S1. Immunocytochemical experiments were performed to confirm the mass spectrometry and biochemical data and assess the cellular distribution of WRP and WAVE. Mouse embryonic fibroblasts exogenously expressing Flag-WRP were stimulated with PDGF and immuno-stained with anti-Flag (red, **A, D, E, H**), anti-WAVE (blue, **B, F, E, H**) and phalloidin (green, **C, G, E, H**). In unstimulated cells the distribution of exogenously expressed WRP was cytoplasmic and clearly distinct from WAVE and actin (data not shown). Cells expressing Flag-WRP at low levels responded normally to PDGF treatment (**A-D**). Upon PDGF stimulation of these cells, a portion of all three proteins appear to co-localize at sites of dynamic actin reorganization including both dorsal ruffles and leading edges. At higher magnification it can be seen that WRP, WAVE and actin are co-distributed at the leading edge

(**E-H**). This co-localization is restricted to regions of the cell where actin nucleation has occurred, consistent with the expectation of a regulated interaction between Rac-activated WAVE and a functional RacGAP. Very high expression levels of exogenous WRP resulted in a generalized decrease in PDGF stimulated ruffling (data not shown), supporting WRP's proposed role as an active RacGAP. Interestingly, the cellular distribution of the WRP W/A mutant appears to remain unchanged upon PDGF treatment and no significant co-distribution with WAVE or actin has been observed (data not shown). When these findings are considered with the interaction data presented in figures 1 and 2 of the manuscript, it seems likely that WRP and WAVE interact at sites of dynamic actin reorganization and via a mechanism that involves the SH3 domain of WRP.

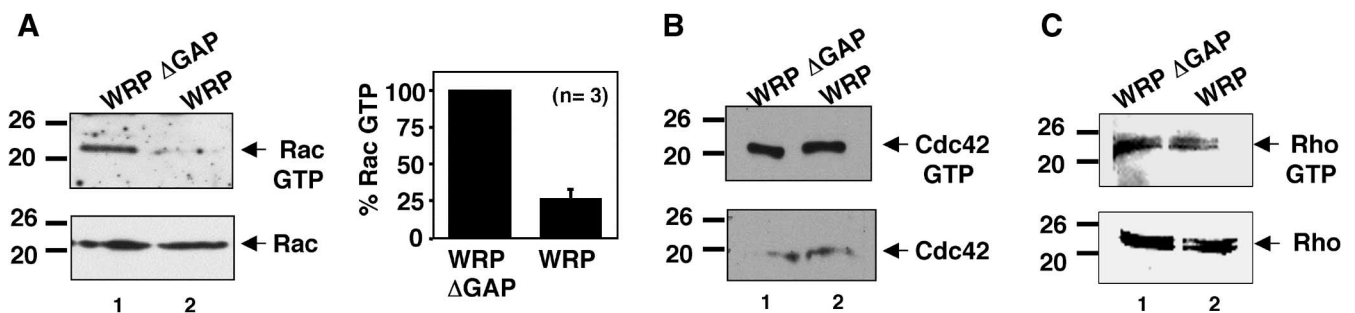


Figure S2. A) HEK293 cells were transfected with WRP or WRP Δ GAP and Rac-GTP levels were measured by the Pak-1 capture assay. Left Top Panel, immunoblot depicting the levels of Rac-GTP captured by the Pak-1 GST fusion protein in WRP Δ GAP (lane 1) or WRP (lane 2) transfected cells. A representative example from three independent experiments is presented. Left Bottom Panel, control experiments demonstrating the levels of endogenous Rac expressed in WRP Δ GAP (lane 1) or WRP (lane 2) transfected cells. The migration position of Rac and the molecular weight markers are indicated in both panels. Right Panel, the levels of Rac-GTP detected in the capture assay were quantified by densitometry using the NIH image program. The amalgamated data (%Rac-GTP) from three experiments is

presented. B-C) HEK293 cells were transfected with WRP or WRP Δ GAP and the Cdc42-GTP levels were measured by the Pak-1 capture assay (B) or Rho-GTP levels by the Rhotekin capture assay (C). Top Panels, immunoblot depicting the levels of Cdc42-GTP captured by the Pak-1 GST fusion protein (B) or Rho-GTP by the Rhotekin capture assay (C) in WRP Δ GAP (lane 1) or WRP (lane2) transfected cells. Bottom Panels, control experiments demonstrating the levels of endogenous Cdc42 (B) or Rho (C) expressed in WRP Δ GAP (lane 1) or WRP (lane 2) transfected cells. The migration positions of Cdc42 and Rho and molecular weight markers are indicated in both panels.

Methods

Immunofluorescence

Mouse embryonic fibroblasts overexpressing WRP were maintained in DMEM supplemented with 10% fetal calf serum. Cultures were serum starved for 12 hours prior to stimulation with human PDGF BB (Peprotech Inc) at a concentration of 50ug/ml for 10 min. Cultures were fixed with 4% paraformaldehyde at room temperature and permeabilized with 0.2% TritonX-100 prior to incubation with anti-FLAG M2 monoclonal antibody (Sigma) to detect exogenously expressed WRP and the anti-WAVE antibody V059 to detect endogenous WAVE. After washing with PBS, cells were incubated with secondary antibodies (Texas Red, Alexa 350 (Molecular Probes)), washed with PBS and stained with phalloidin (Oregon Green (Molecular Probes)). Cells were mounted with Geltol Mounting Medium (Thermo Shandon) and visualized with a Leica DM IRE2 system.

Pak1 and Rhotekin Capture Assay

Cellular WRP activity in HEK293 cells was measured by a modification of the PAK pull-down assay of X.D. Ren and M.A. Schwartz (Ren, X. D. & Schwartz, M. A. *Methods Enzymol* 325, 264-272 (2000)). The CRIB domain of PAK-1 was PCR cloned as above and subcloned into pGEX4T1 to generate a GST fusion protein. HEK293 cells (4 X 10⁶ cells) were transfected with WRP (4 µg) or control vectors using Lipofectamine Plus (BRL). After 24 hours, plates were washed with cold PBS and lysed in 50 mM Tris, pH 7.2, 1% Triton X-100, 0.5% sodium deoxycholate, 0.1% SDS, 500 mM NaCl, 10 mM MgCl₂. The homogenates were then centrifuged at 15,000 rpm for 15 min at 4°C and the supernatants were incubated with 30 µg of GST-PAK1 or GST-RBD (Upstate) immobilized on glutathione sepharose for 45 min at 4°C. The pellets were resuspended in 30 µl of 2X Laemmli sample buffer and separated by SDS-PAGE on 4-15% gradient gels. Levels of bound Rac, Cdc42 and Rho were determined by western blotting using specific antibodies for Rac-1 (Transduction Lab), Cdc42 (Santa-Cruz), or RhoA (Santa-Cruz).